The 2012 World Congress on
Advances in Civil, Environmental, and Materials Research (ACEM' 12)
Seoul, Korea, August 26-30, 2012

Effect of Fines Content on the Small Strain Stiffness of Sand

X. Liu[1] and *J. Yang[2]

[1), 2)] *Department of Civil Engineering, The University of Hong Kong, Hong Kong*
[2)] *junyang@hku.hk*

ABSTRACT

A series of resonant column (RC) and bender element (BE) tests was carried out at different stress levels to investigate the small strain shear stiffness of a mixture of clean quartz sand and crushed silica fines, with focus on the effect of fines content. All specimens were prepared by the moist tamping method at a similar initial global void ratio and tested under saturated conditions. The test results show that the G_0 value of the mixture increases with confining stress and meanwhile the increase of fines content continuously decreases the G_0 value at a certain stress level. Comparing the measurements from two different test methods, G_0 values obtained from the bender element tests are much higher than the corresponding ones from the resonant column tests (about 20%), whereas for the clean quartz sand the G_0 values measured by the two methods were found to be consistent with each other.

1. INTRODUCTION

The shear stiffness of soil within a narrow range of shear strain (i.e., $\gamma < 0.001\%$) is known as the small strain shear stiffness, and often denoted as G_0 or G_{max}. In the past decades, numbers of studies have been performed with focus on various factors affecting this important soil property, such as effective stress level, void ratio, loading history, particle size distribution, and saturation conditions (e.g., Iwasaki & Tatsuoka, 1977; Seed *et al.*, 1986; Youn et al., 2008; Wichtmann & Triantafylidis, 2009; Yang & Gu, 2011). Most of these studies used clean granular materials due partly to the difficulties in sampling and transportation of natural sand deposits (Carraro *et al.*, 2009; Chien & Oh, 2002). By using the resonant column apparatus, Iwasaki & Tatsuoka (1977) investigated the small strain stiffness of clean sand, natural sand, and artificially graded sand, showing the influence of fines content. Recently, Salgado *et al.* (2000) studied the small strain shear stiffness of silty sand based on the measurement from bender element tests. Using the same technique, Carraro *et al.* (2009) performed tests to investigate the influence of

[1)] Graduate Student
[2)] Associate Professor

plasticity to the G_0 value by adding non-plastic silt and kaolin clay into clean Ottawa sand. It is widely recognized that data interpretation using the bender element method involves many uncertainties (Jovicic *et al*., 1996; Lee & Santamarina, 2005; Sanchez-Salinero *et al*., 1986). Particularly for granular materials, the characteristics of signals are found to be complicated, depending on a number of factors such as particle size, frequency, confining pressure and packing density (Yang & Gu, 2012).

By taking advantage of the new testing system set up at the University of Hong Kong (HKU), a series of resonant column (RC) and bender element (BE) tests was able to be conducted on the same specimens formed by mixing Toyoura sand with crushed silica fines of varying quantities. The effects of fines and test method to the small strain stiffness of the soil can be assessed by comparing the results from both test methods. Besides, the output signals from bender element tests with respect to different fines content were also investigated.

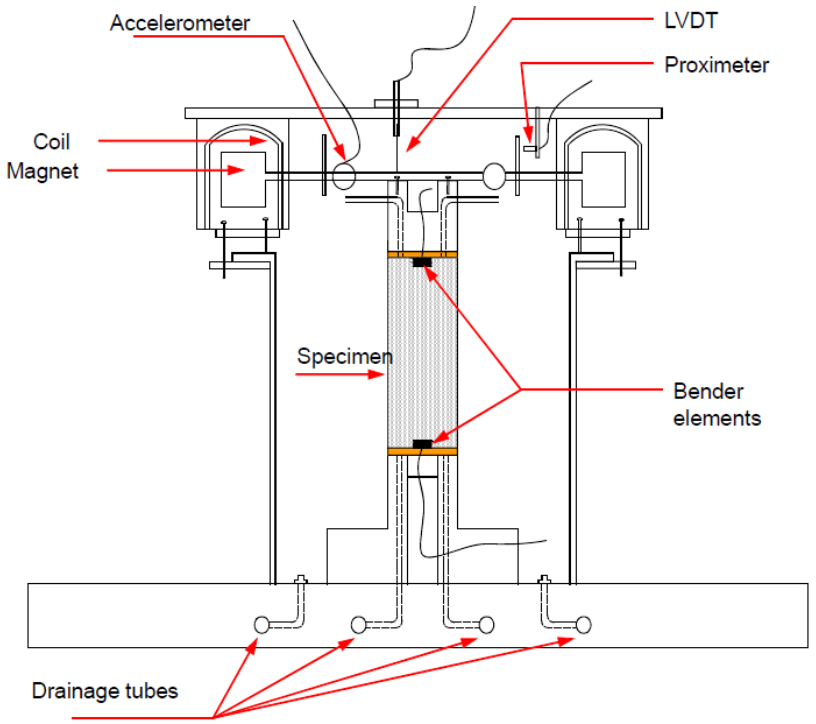

Fig. 1 Schematic set up of the testing system at HKU

2. TEST EQUIPMENT AND MATERIAL

2.1 Test apparatus

Two different types of resonant column apparatus have been widely used as the “fixed-free” type (Stokoe type), and the “free-free” type. In this study, the Stokoe type of resonant column apparatus was used and the schematic set up of the testing system is illustrated in Fig. 1. The apparatus includes a loading cell with capacity up to 1 MPa, a drive head with four magnets placed inside the coils, a top cap with porous stone, and a pedestal inside a water bath

chamber. The internal LVDT is installed to measure the axial displacement with time. To generate the shear wave, a pair of bender element was installed on the top cap and pedestal as the transmitter and receiver, respectively. Each piezoelectric element is 11 mm in width and 1.2 mm in thickness with a penetration depth of 2.0 mm. In order to prevent the “crosstalk” (Lee & Santamarina, 2005), two piezoelectric elements are shielded with polyurethane coating, and then grounded.

2.2 Test materials and sample preparation

In this study, the Toyoura sand was mixed with the silt-sized crush silica at different contents. The particle size distribution curves of the mixtures are shown in Fig. 2, and the basic material properties are summarized in Table 1.

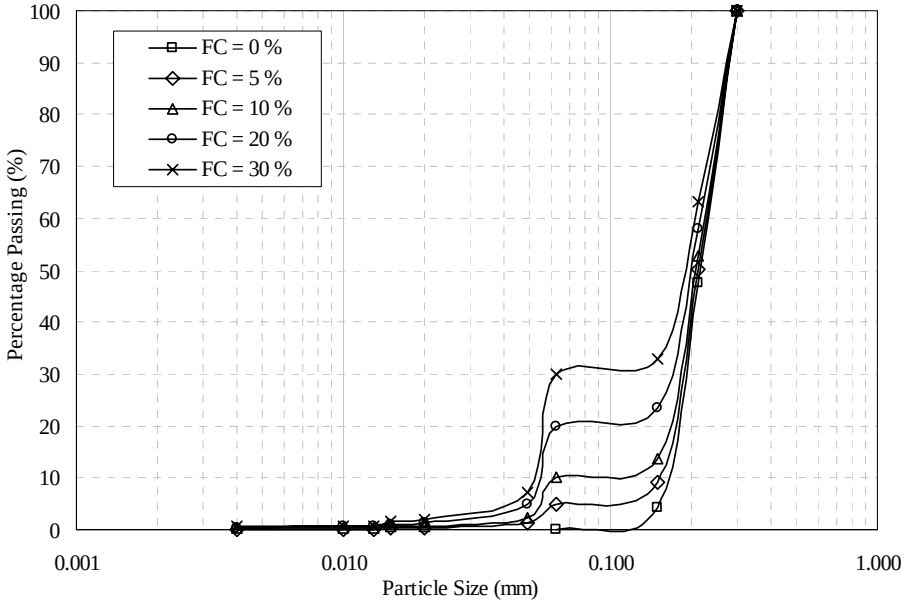

Fig. 2 Size distribution curves of mixtures with different fines contents

Table 1 Properties of test materials

	Toyoura sand	Crushed silica
G_s	2.65	2.63
e_{max}	0.967	-
e_{min}	0.633	-
C_u	1.392	2.08
D_{50}	0.216 mm	0.057 mm

All test specimens were prepared at 100 mm in height and 50 mm in diameter by moist tamping (MT) method. The reasons of using MT are to overcome the segregation of the Toyoura sand with fines and to prepare the

possible loosest specimen. The general procedure of the MT method consisted of the continuous compaction of several separated layers under a quasi-static load. During the sample preparation, the surface of each layer was scratched with a steel ruler so that it had a good contact with the succeeding layer. Because of the difficulty in determining the relative density of the mixed material with fines, a global void ratio was adopted as the target in this study (e = 0.865). Upon the completeness of sample preparation, a stand-up suction of 25 kPa was applied to the soil specimen. The sample was then flushed with CO_2 and de-aired water. A back pressure of 350 kPa was applied to the specimen to ensure saturation of the specimen. *B*-check was performed afterwards and *B*-value greater than 0.95 was obtained for all specimens (BS-1377). The isotropic confining pressures were then applied in five steps to the specimen as 50 kPa, 100 kPa, 200 kPa, 400 kPa, and 500 kPa. During each loading stage, 30 minutes of consolidation was allowed, and the finish of consolidation was monitored by continuous checking the LVDT measurements. At the end of each loading step, both the RC and BE tests were performed.

3. TEST RESULT AND DISSCUSION

3.1 Signal interpretation

In the BE test, the small strain shear modulus of the soil specimen can be estimated by applying the elastic wave theory, as

$$G_0 = \rho * V_s^2 \tag{1}$$

Where ρ is the mass density and V_s is the shear wave velocity.

By analyzing the output signal from the BE test, the shear wave speed can be calculated as

$$V_s = \frac{L}{t} \tag{2}$$

Where *L* is the travel distance between two tips of the piezoelectric elements, and *t* is the travel time, often denoted as the first arrival time of the shear wave.

Although the bender element receives considerable interest over the past years due to its small disturbance to the soil specimen (i.e., $\gamma < 0.001\%$) and to the convenience of incorporating it into various soil testing devices, the interpretation of wave signals still remains controversial because of the difficulties in estimating the travel time (Jovicic *et al.*, 1996; Lee & Santamarina, 2005). In this study, an input sinusoid signal with a very wide range of frequencies (from 1 kHz to 80 kHz) was generated. The output signals were then able to be assessed in a whole view under different input frequencies, thus leading to an increased reliability of data interpretation and a better understanding of the characteristics of signals (Yang & Gu, 2010; 2012).

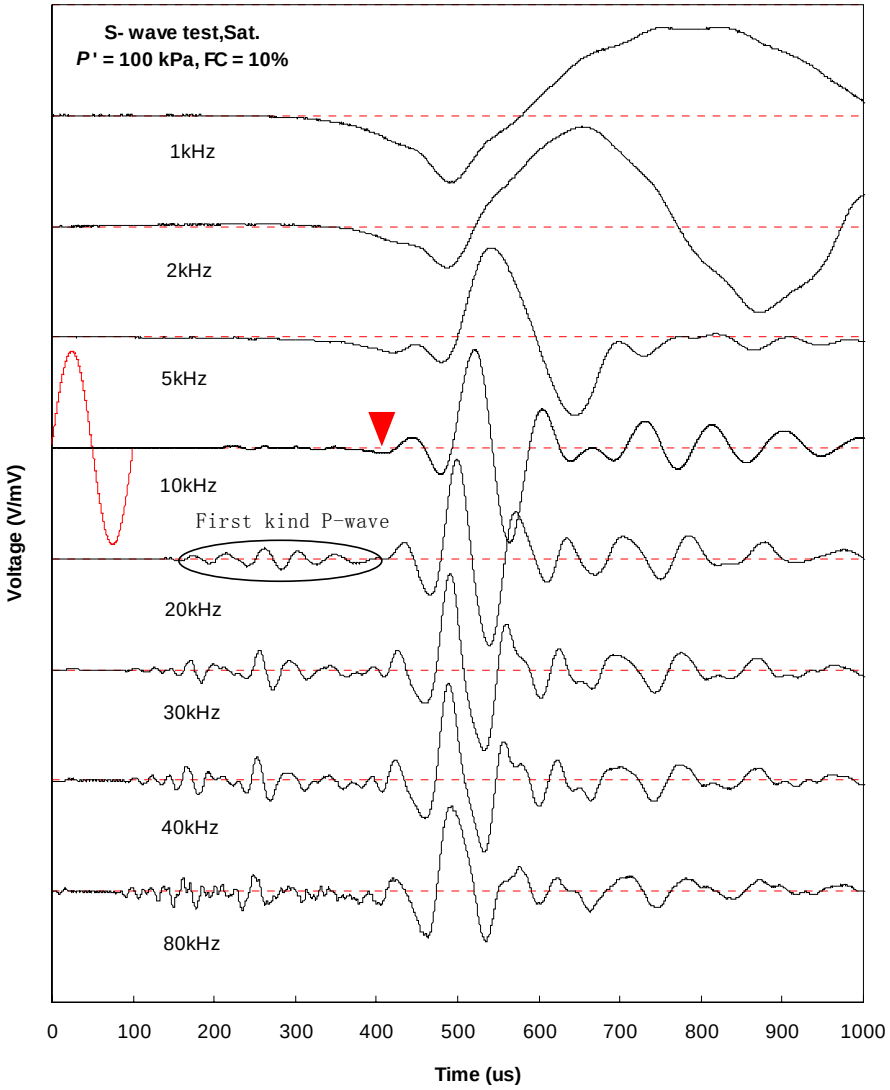

Fig. 3 Output signals at different frequencies in saturated condition

Fig. 3 shows a series of shear waveforms generated for a saturated specimen with 10% fines content under an effective confining stress of 100 kPa. By comparison, the received signals with frequencies smaller than 10 kHz are very different in shape. Whereas, the output signals at higher frequencies have similar shapes for both the first kind P-wave as well as the major shear wave. Evidently, the waveform of the output signal is frequency dependent in that the received signal contains more high-frequency components as the input frequency increases. Besides, the near field effect is obvious when the input frequency is less than 10 kHz and gradually diminishes with greater input frequencies. As a whole, the received signal at an input signal of 10 kHz is clear and thus much easier to determine the first shear wave arrival. This is possible due to that the input frequency of 10 kHz is close to the resonant frequency of the bender element itself (Jovicic *et al.*, 1996). Therefore, the possible arrival time of the shear wave is marked as the downward triangle at

10 kHz which is defined as the second downward deflection point before the major peak based on the start to start method.

3.2 Effect of fines content to the BE signal

To examine the effects of fines to the BE signal, the output signals with input frequency of 10 kHz at different fines content are plotted at the effective confining stress of 100 kPa in Fig. 4. Again, at the input frequency of 10 kHz, the waveforms are similar in shape where a small peak exists followed by the major peak. However, existence of fines turns to lower the output frequency, especially at low confining stress (i.e., σ' = 100 kPa). Besides, comparing with the main shear wave, the first kind P-wave attenuates much faster; this finding is supported by the study of Sanchez-Salinero *et al*. (1986).

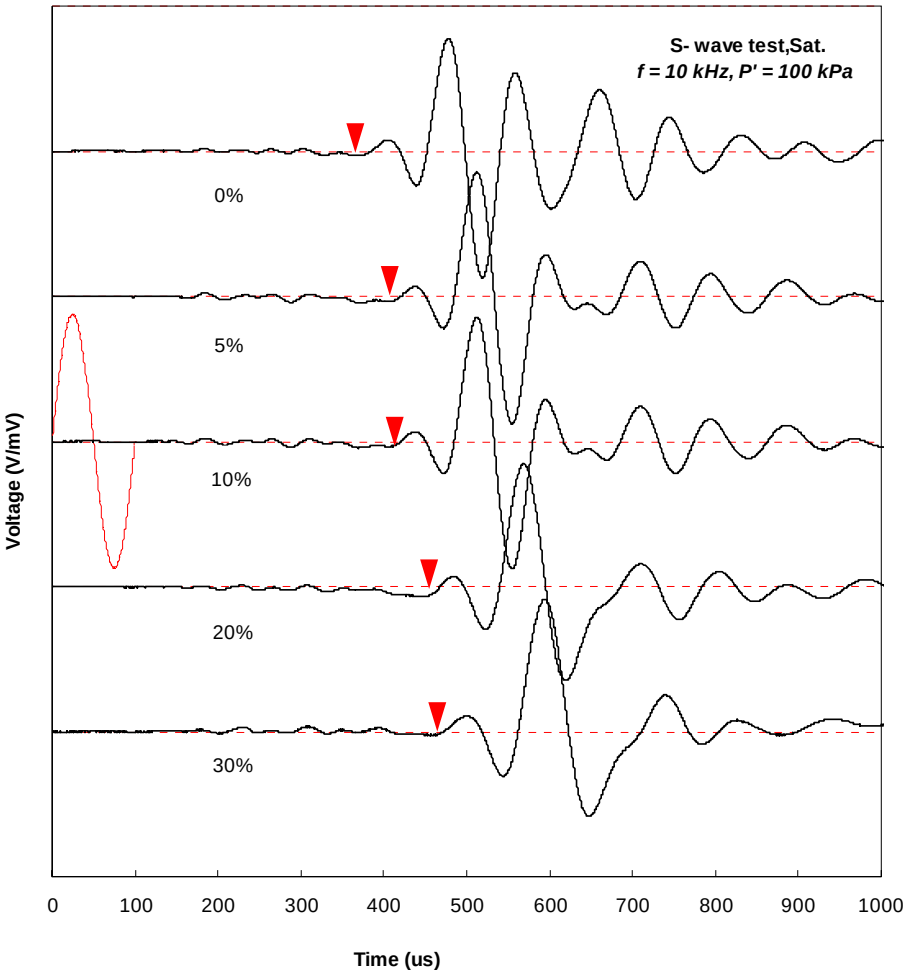

Fig. 4 Output signals at different fines contents in saturated condition

3.3 Effect of fines content to the RC measurement

In the RC test, the soil specimen is confined within the membrane between the top and bottom caps. By subjecting a forced vibration from the driving arm with certain amplitude and frequencies, the resonant frequency of the specimen can be found when plotting the response of the driving head with a range of input frequencies. Then, the elastic wave propagation theory (Eq. 1)

was applied to determine the G_0 value, where the shear wave velocity can be calculated from the resonant frequency.

In this study, empirical equation (3) suggested by Hardin & Richart (1963) was used to fit the test measurements:

$$G_0 = AF(e)\left(\frac{\sigma'}{P_a}\right)^n \quad (3)$$

Where σ' is the effective confining stress; P_a is the atmospheric pressure; A and n are fitting parameters; and $F(e)$ is the void ratio function accounting for the effect of void ratio as:

$$F(e) = \frac{(2.17 - e)^2}{1+e} \quad (4)$$

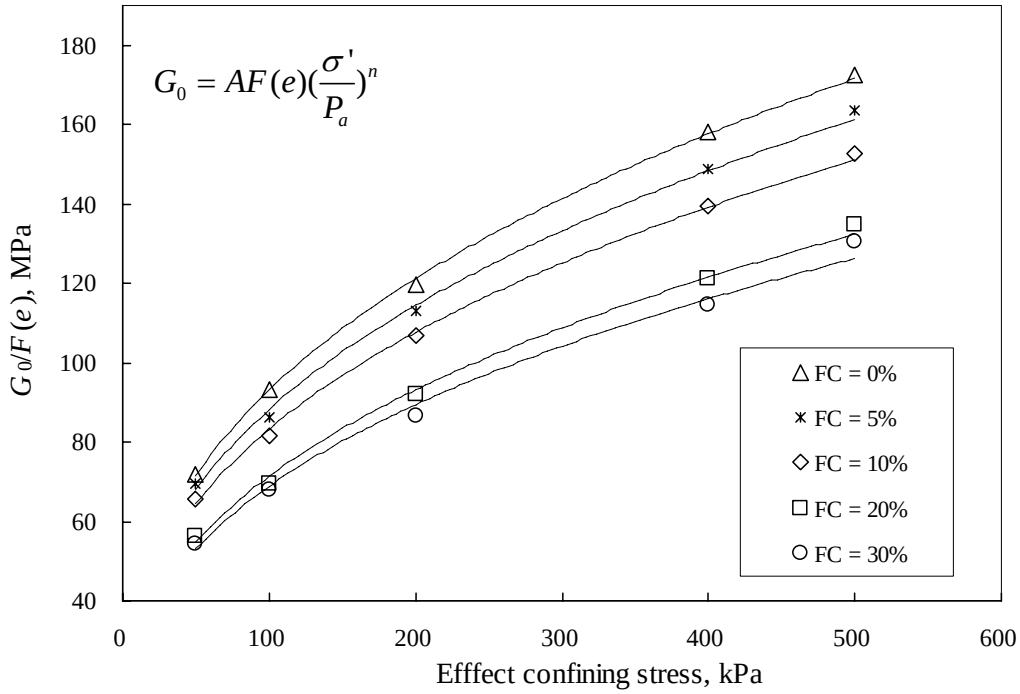

Fig. 5 Variation of G_0 values at different confining stresses

Fig. 5 shows the normalized small strain shear modulus obtained by RC tests against the effective confining stress. At each fines content, the test measurements were fitted by Eq. 3. Evidently, the G_0 value increases with the confining stress, and the increase of fines content tends to reduce the small strain stiffness. To obtain a better view of the effects of fines to the small strain stiffness, the normalized small strain shear modulus was also plotted against fines content at different confining stresses in Fig. 6. Again, the small strain shear modulus initially drops quickly when the fines content is less than 20%, especially at higher confining stress, say, σ' = 500 kPa. However, a smaller reduction of G_0 value can be observed when the fines content becomes greater.

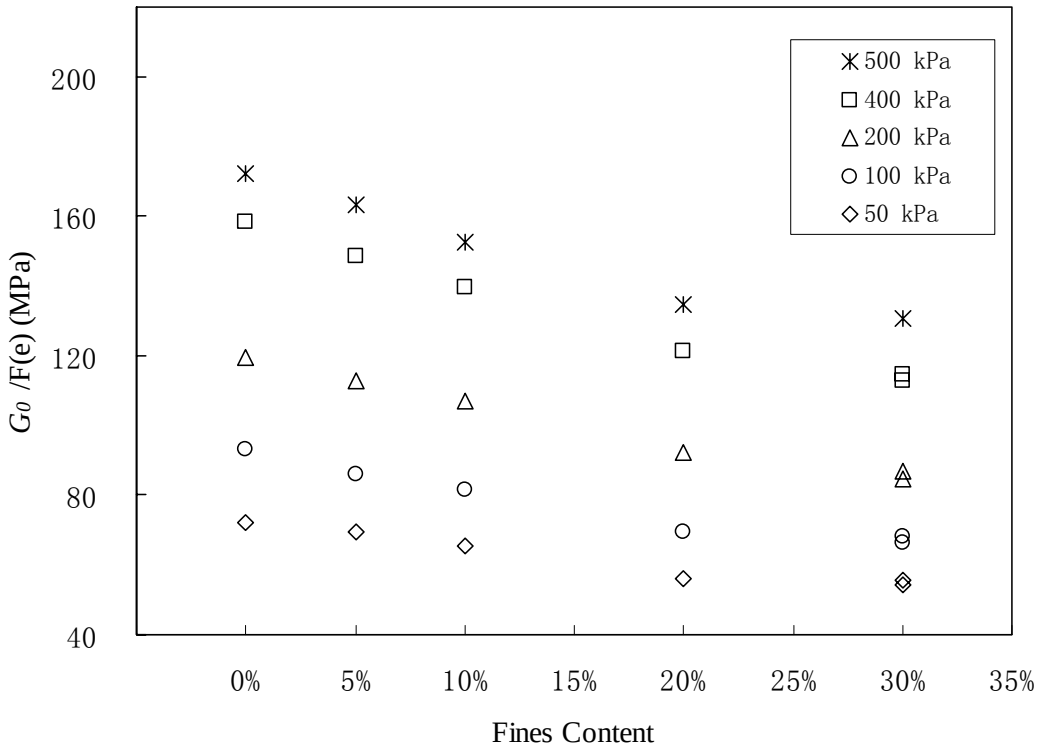

Fig. 6 Variation of G_0 values at different fines content

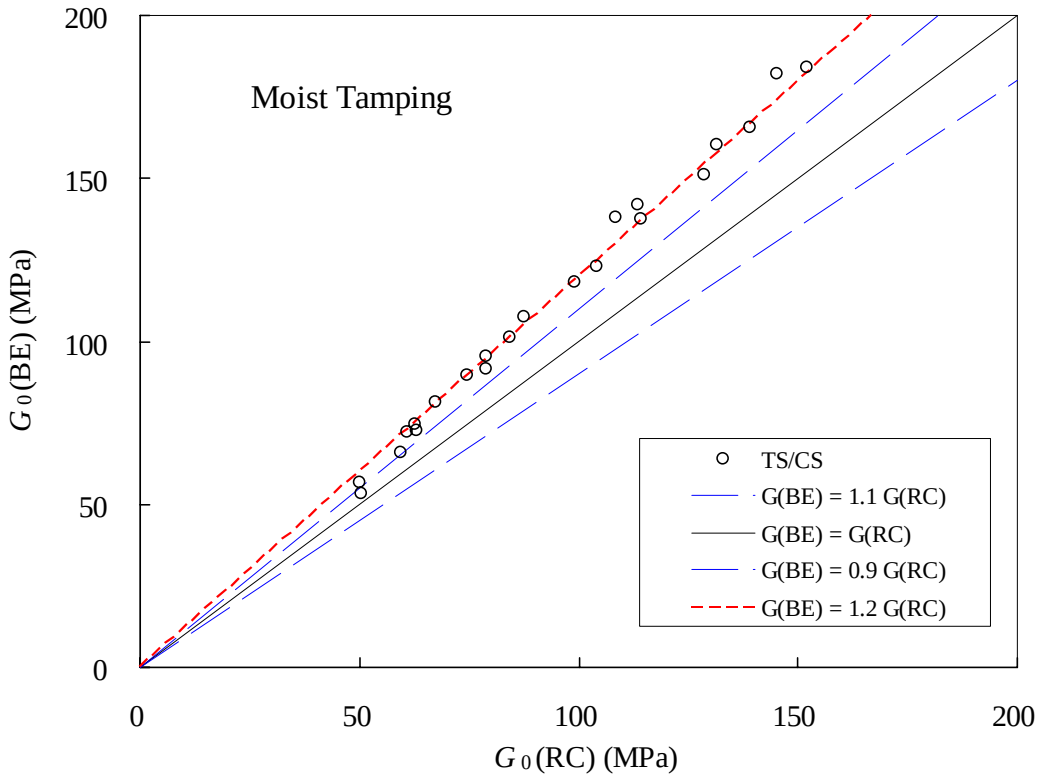

Fig. 7 Comparison of G_0 values from BE and RC tests

Table 2 Fitting parameters by Eq. 3

Fines Content	Test method	Fitting parameters		
		$F(e)$	A	n
0%	BE	$(2.17\text{-}e)^2/(1+e)$	19.76	0.38
	RC		16.23	0.38
5%	BE	$(2.17\text{-}e)^2/(1+e)$	16.41	0.40
	RC		15.73	0.37
10%	BE	$(2.17\text{-}e)^2/(1+e)$	14.36	0.41
	RC		15.13	0.37
20%	BE	$(2.17\text{-}e)^2/(1+e)$	13.06	0.40
	RC		12.23	0.38
30%	BE	$(2.17\text{-}e)^2/(1+e)$	12.54	0.40
	RC		12.16	0.38

3.4 Comparison of RC and BE measurements

As shown in Table 2, the fitting parameters from BE tests seem to be slightly greater than those from the RC tests, which indicates that the stiffness measured from BE tests is greater than that from RC tests. At the meanwhile, the parameter "A" decreases with fines content for both BE and RC tests, which indicates a reduction of the small strain stiffness with fines content. In Fig. 7, the G_0 values from the BE and RC tests are compared. The discrepancy is about 20%. It is worth noting, however, that for the clean quartz sand, the G_0 values measured by RC and BE methods were quite consistent with each other (Gu & Yang, 2011), implying the dependence of the test method effect on particle gradation.

4. CONCLUSION

In this study, the resonant column test and the bender element test were conducted on the mixture of Toyoura sand with crush silica fines at different fines contents. All tests were performed under a sequence of loads with the same initial global void ratio. The first arrival time of the shear wave was determined within a wide range of input frequencies, and the input frequency of 10 kHz turned out to be an optimal frequency giving a reliable estimation. The shape of the output waveform was frequency dependent that higher input frequency tended to produce high frequency components. The variation of the fines content had little effect on the waveform of the output signal except to reduce the output frequency. On the other hand, the G_0 value increased with the confining stress, and decreased with the fines content. The reduction was much clear at low fines content. Moreover, an important finding was obtained by comparing the results from BE and RC tests that the small strain stiffness measurements in BE tests were about 20% higher than those in the corresponding RC tests but they were quite consistent with each other for the

same clean sand.

ACKNOWLEDGMENT

The financial support provided by the University of Hong Kong under the Seed Funding for Basic Research scheme and through the Research Output Prize is gratefully acknowledged. The first author thanks X.Q. Gu for his help during the test program.

REFERENCE

Carraro, J., Prezzi, M., and Salgado, R. (2009), “Shear strength and stiffness of sands containing plastic or noplastic fines.” *J*. *Geotech*. *Geoenviron. Eng., ASCE,* Vol. **135**(9), 1167-1178.

Chien, L. K. and Oh Y. N. (2002), “Influence of fines content and initial shear stress on dynamic properties of hydraulic reclaimed soil.” *Can. Geotech. J.* Vol. **39**, 242-253.

Gu, X.Q. and Yang, J. (2011), “Laboratory measurement of shear stiffness of decomposed granite.” *Proc*. *the 14th European Conference on Soil Mechanics and Geotechnical Engineering,* Athens, Greece.

Hardin, B. O. and Richart, F. E. (1963), “Elastic wave velocities in granular soils.” *Journal of Soil Mechanics and Foundation Engineering Division, ASCE,* Vol. **89**(SM1), 39-56.

Iwasaki, T. and Tatsuoka, F. (1977), “Effect of grain size and grading on dynamic shear moduli of sand.” *Soils and Foundations,* Vol. **38**(1), 19-35.

Jovicic, V., Coop, M. R. and Simic, M. (1996), “Objective criteria for determination of G_{max} from bender element tests.” *Géotechnique*, Vol. **46**(2), 357-362.

Lee, J. S. and Santamarina, J. C. (2005), “Bender elements: performance and signal interpretation.” *J*. *Geotech*. *Geoenviron. Eng., ASCE,* Vol. **131**(9), 1063-1070.

Salgado, R., Bandini, P., and Karim, A. (2000), “Shear strength and stiffness of silty sand.” *J*. *Geotech*. *Geoenviron*. *Eng, ASCE*, Vol.**126** (5), 451- 462.

Sanchez-Salinero, I., Roesset, J. M. and Stokoe, K. H. II. (1986), “Analytical studies of body wave propagation and attenuation.” Report No. GR-86-15, Univ. of Texas, Austin, Texas.

Seed, H. B., Wong, R. T., Idriss, I. M., and Tokimatsu, K. (1986), “Moduli and damping factors for dynamic analyses of cohesionless soil.” *J. Geotech*. *Geoenviron*. *Eng.*, *ASCE,* Vol. **112**(11), 1016–1032.

Wichtmann, T. and Triantafyllidis, Th. (2009), “Influence of the grain-size distribution curve of quartz sand on small strain shear modulus G_{max}.” *J. Geotech*. *Geoenviron*. *Eng*., *ASCE*. Vol. **135**(10), 1404-1418.

Yang, J. and Gu, X.Q. (2010), “Dynamic shear modulus of dry sand: effect of test method,” *Proc*. *14th European Conf. Earthquake Eng.*, Ohrid, Macedonia.

Yang, J. and Gu, X. Q. (2011), “Measurement of shear waves in dry and saturated sand.” *Proc*. *14th Asian Regional Conference on Soil Mechanics and Geotechnical Engineering*, Hong Kong.

Yang, J. and Gu, X. Q. (2012), “Shear stiffness of granular material at small strains: does it depend on grain size?” *Géotechnique*, in press.

Youn, J.-U., Choo, Y.-W. and Kim, D.-S. (2008), “Measurement of small-strain shear modulus G_{max} of dry and saturated sands by bender element, resonant column, and torsional shear tests.” *Can. Geotech. J.,* Vol. **45** 1426-1438.